On size effect in tension of SFRC thin plates

Marco di Prisco, Roberto Felicetti, Marco G.L. Lamperti, Giovanni Menotti
Department of Structural Engineering, Politecnico di Milano, Italy.

ABSTRACT: More than 48 SFRC thin plates characterized by a central notch (notch ratio = 0.2), a high-strength matrix (f_c = 75 MPa) and two different types of steel fibers, were tested in tension. Three sizes were considered (1 : 2.5 : 6.25). They were subjected to uniaxial tension (rotating-end platens), eccentric tension, and 4-point bending. Each test was repeated three times. The material characterization was performed by means of direct tension tests (notched specimens) and 4-point bending tests (unnotched specimens); three unnotched large slabs were also tested according to a 4-point bending test procedure. The tests highlight both the deterministic and the statistical size-effect. The results show a significant difference between uniaxial tension and bending with reference to post-cracking behavior. By adopting a plane-section kinematic model and a constitutive law identified on the basis of unnotched 4-point bending procedure, the whole set of tests was reproduced to validate a linear softening constitutive model and to discuss the application limits for design.

Keywords: material characterization, steel fibers, fracture, size-effect, bending, tension

1 INTRODUCTION

1.1 *Size effect in SFRC structures*

Steel Fiber Reinforced Concrete is a material characterized by a residual stress after cracking, when subjected to uniaxial tension. This feature ensues from fiber pull-out and depends on fiber-matrix interaction, number of active fibers and fiber distribution. For economical reasons, the amount of fiber, commonly used in civil structures, is limited to 1% by volume and this implies a softening behavior in uniaxial tension. Therefore, fiber stabilizes crack propagation, but for fiber amount not exceeding 1% by volume, the peak behavior in uniaxial tension is not significantly changed by fiber addition, while the post-peak behavior grows linearly with fiber amount.

On the contrary, bending behavior exhibits larger toughness, owing to the linear distribution of strain in the section between two cracks. The peak strength in bending can be close to the residual strength at large crack opening w ($0.5 < w < 1.5$ mm) and, therefore, it is interesting to understand how size effect affects both the peak strength of the matrix and the residual value for large crack openings, due to fiber pull-out. If the former should be more reduced than the latter, a more ductile behavior could expected for large SFRC structures compared to small structures, as in R/C bent structures.

The current research (Bažant 2002, 2003) is oriented to consider size-effect mainly due to two physical reasons. The balance between fracture energy (associated to a critical volume having the crack surface as a basis and the material characteristic length as a depth, whose value is close to the aggregate maximum size) and elastic energy release (that is proportional to the volume of the structure involved by crack propagation) cause the "deterministic" size-effect, that mainly affects the peak of the matrix strength (van Vliet 2000). On the other hand, the influence of defects, according to Weibull's theory (Weibull 1951) grows with the size of the structure and causes the "statistical" size effect. The former significantly reduces the peak strength for limited structure size and acts mainly on the crack propagation in the matrix; the latter also acts on the matrix peak, prevailing for large structures, but it also affects the residual behavior controlled by steel fiber pull-out, that is character-

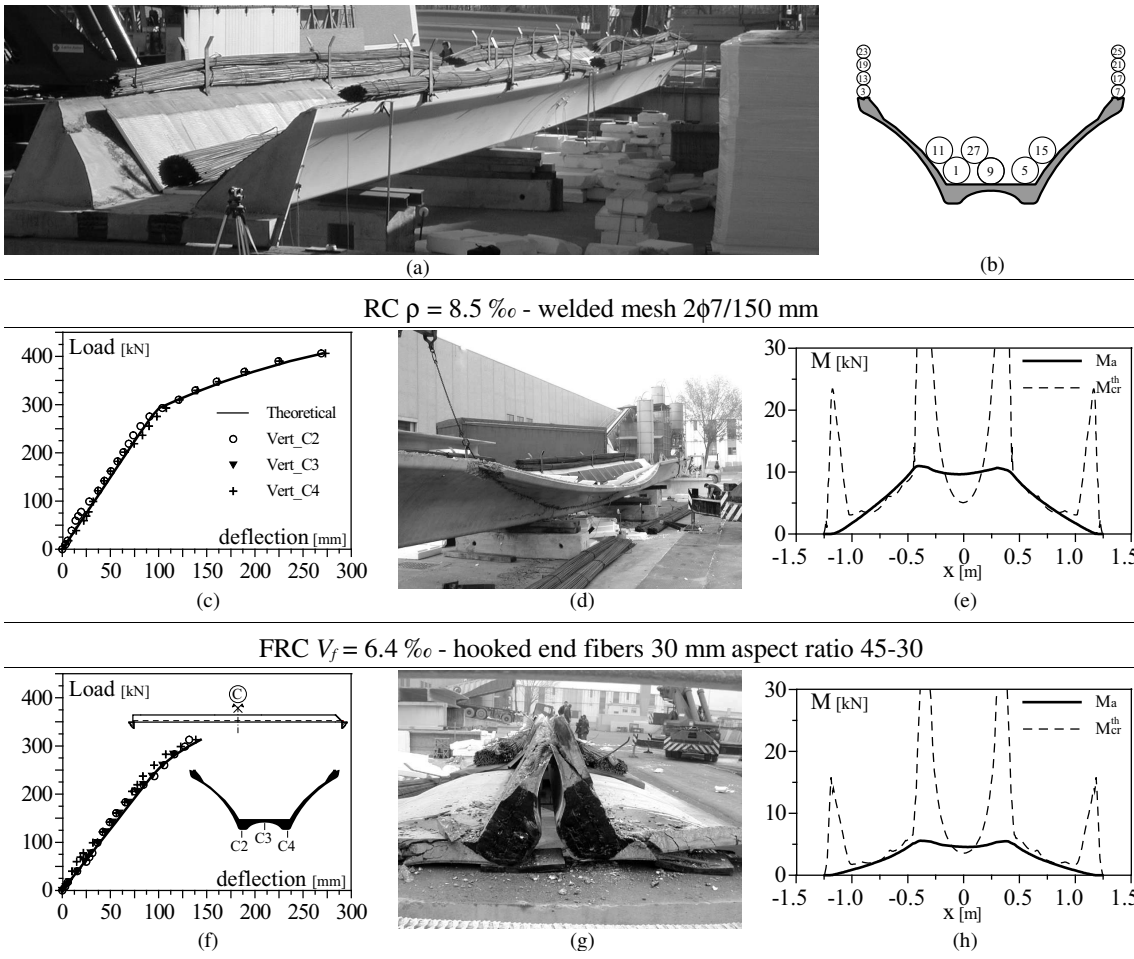

Figure 1. Precast roof elements 30 m long and 2.5 m wide (a), simply supported and loaded by means of steel rebar bundles (b); load-deflection curves (c,f); failure modes (d,g); transversal bending moment (e,h).

ized by a very high scatter compared with that measured in plain concrete.

1.2 *The engineering problem*

The interest in this topic is connected to the design of thin-webbed SFRC precast roof elements (di Prisco 2000, di Prisco et al. 2000a, 2003). These structures have a span of up to thirty meters (Fig. 1a), they are longitudinally prestressed in the bottom chords, and conventionally reinforced only at the end, in the diffusion zones close to the supports. The diffused transversal reinforcement, traditionally made of welded steel fabric, is replaced by steel fiber reinforcement. This structure is designed to fail in longitudinal bending, but snow loads, acting as distributed loads on the extrados and as concentrated loads linearly distributed along the skylights supports on top chords, induce a transversal bending moment and an axial tensile force due to the inclination of the two wings. The combination of these actions cause a transversal eccentric tension in the longitudinal cross section along the plane of symmetry with an eccentricity value close to the thickness of the plate. This action remains quite constant along the whole span of the element (di Prisco et al. 2000a), pointing out a significant benchmark to investigate both the deterministic and the statistical aspects of size-effect.

In Figure 1 the structural behavior up to collapse of these structures is shown. Each element reaches cracking along the central longitudinal section, just after the onset of transversal cracking due to longitudinal bending. The longitudinal cracking is justified not only by the strength reduction caused by size-effect, but also by a second-order effect that increases the transversal bending moment M_a of about 30% in the central region (where the longitudinal curvature exceeds the cracking value - Figs. 1 e, h; di Prisco et al. 2002). After the transversal cracking, only the r/c element shows a progressive

opening of the two inclined wings (up to 90 mm) at increasing load up to collapse. Despite the second order effect and the cross-section shape loss, the experimental maximum load was only 6% less than the theoretical prediction. By contrast, SFRC elements showed a brittle failure owing to the unstable crack propagation along the central longitudinal section.

1.3 *The linear constitutive model for design*

Fiber increases the residual tensile strength of the material after cracking. Although the tensile stress versus Crack Opening Displacement (COD) curve sometimes exhibits a hardening branch for high-carbon steel fiber, the simplicity requirements imposed by design suggest the adoption of a linear branch (Fig. 2). Therefore, according to r/c structure design, the tensile contribution of concrete matrix in bending is neglected.

Several experimental tests have ascertained a large influence of fiber dispersion and cast modalities on thin plate tensile behavior. For this reason the identification procedure here suggested takes the unnotched 4-point bend thin plate as a reference (60 mm thick). Its introduction is essentially aimed to take into account the real orientation factor and to better evaluate the post-peak strength, especially when multi-localization effects are expected; it allows the designer to more accurately estimate the ultimate capacity for an assigned ductility.

The linear post-cracking behavior is defined on the basis of two points related to Service and Ultimate Limit State respectively. The nominal stress in the COD range of 0.3 mm ± 20% (Fig. 2a) is assumed as a reference for the former value, while the latter is directly related to the nominal stress corresponding to an assigned rotational capacity (φ = 0.02 rad).

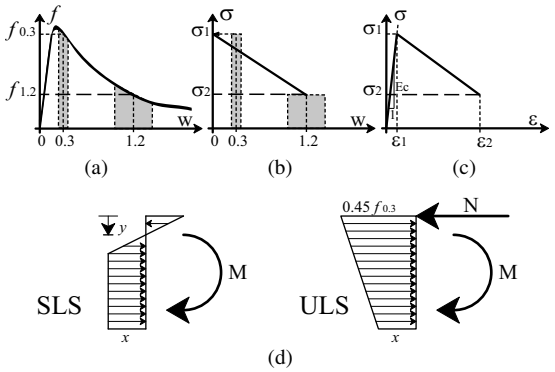

Figure 2. Linear post-cracking model: (a) equivalent-stress vs. crack-opening experimental curves; (b,c) discrete and smeared tensile constitutive curves; (d) assumed stress distributions.

For a bent SFR plate of thickness h = 60 mm the ultimate crack width is $w_u = 0.02 \cdot h$, and the reference nominal stress is computed as the mean value in the range of w_u = 1.2 mm ± 20%. The relation between the tensile stress and the nominal stress identified for both the points is based on equilibrium. An elasto-plastic tensile distribution for the S.L.S. and a compression force concentrated on the top fiber for the U.L.S. are assumed (Fig. 2d). The resultant relations become:

$$\sigma_1 = 0.45\, f_{0.3}$$
$$\sigma_2 = 0.50\, f_{1.2} - 0.225\, f_{0.3} \quad (1)$$

The post-cracking stress-strain relation in uniaxial tension is finally identified by dividing the crack opening w by the structural characteristic length l_{cs}, that can be assumed equal to the beam depth h (di Prisco et al. 2000b, 2001). An initial elastic branch up to the stress σ_1 completes the constitutive behavior of the smeared-crack localized continuum.

2 THE EXPERIMENTAL PROGRAM

The whole set of specimens characterized by a thickness of 60 mm was obtained by sawing casted concrete plates 525 × 940 × 60 mm. The mix design of the matrix is resumed in Table 1. Two materials were analyzed. They had the same HPC matrix (f_{ck} = 75 MPa) and were both reinforced with 50 kg/m^3 of 30 mm long hooked-end steel fibers: the fibers were made of low or high-carbon steel and were characterized by two different aspect ratio (45 or 80 respectively).

Beside characterization tests, more than 25 prismatic centrally notched specimens (notch ratio = 0.2) for each material were tested. They were characterized by the same thickness (60 mm) and three sizes (1 : 2.5 : 6.25), being the smallest specimen 84 mm wide and 150 mm long. They were subjected to uniaxial tension (rotating-end platens), eccentric tension (e = 60 mm), and 4-point bending.

Table 1. Concrete mix design.

Component	quantity/m^3
Cement I 525 R	380 kg
Fly ash	60 kg
Sand 0-3 mm	120 kg
Sand 0-12 mm	970 kg
Gravel 8-15 mm	815 kg
Acrylic superplasticizer	3.5 l
Total water	150 l

Each test was repeated three times. Finally, three unnotched slabs made of low-carbon steel-fiber material (750 × 150 × 60 mm) were also tested according to a 4-point bending procedure.

2.1 *Material characterization*

The characterization of the mechanical properties was carried out by means of 4-point bending tests on 60 mm thick unnotched specimens (150 × 60 × 600 mm; Figs. 3a, b).

In the material identification procedure, the curve characterized by the largest toughness in the low-carbon SFRC specimens was not taken into account because it was regarded as anomalous even if the scatter obtained was confirmed by further experiments. Moreover, one high-carbon SFRC specimen was not suitably controlled.

The choice of the depth (60 mm) corresponds to the average value of the precast roof cross section profile. Also 4-point bending tests (6 for each material, according to UNI Italian Specification; 150 × 150 × 600 mm; notch ratio = 0.3), and fixed-end uniaxial tension tests (prismatic specimens, 60 mm thick; notch ratio = 0.2) were carried out on notched specimens.

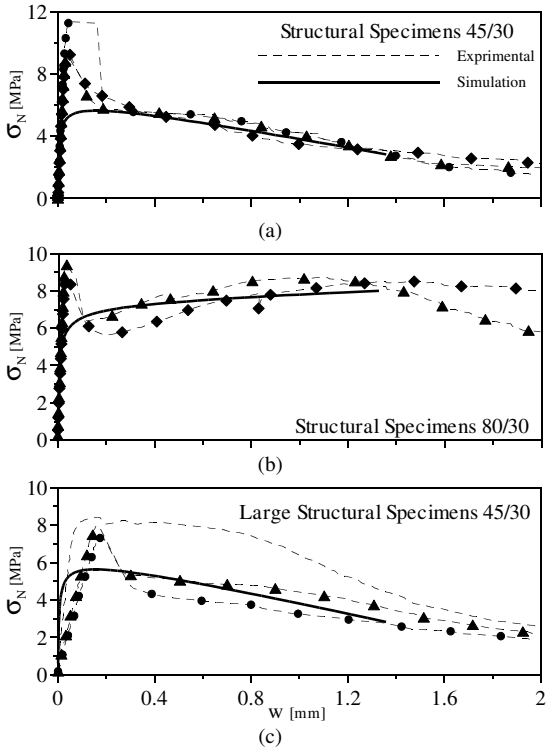

Figure 3. 4-point bending on unnotched thin plates: (a,b) structural tests for material characterization, (c) 45-30 large structural specimens

The UNI test is very similar to the RILEM test: it is a four-point instead of a three-point bend test and its notch-ratio is greater (0.3 vs. 0.17), the cross section of the specimen is the same (150 × 150 mm), and the span is slightly shorter.

A comparison between the two specimens revealed only a weak difference on the peak-load, the four-point bend test always provides a lower strength (Ferrara & di Prisco 2001). The experimental results (Fig. 4a, b) highlight how the presence of a notch involves a post-cracking hardening and a larger scatter of the experimental results, compared to unnotched bending tests on thinner specimens.

The comparison with the theoretical behavior, computed by means of the linear post-cracking constitutive curve and a plane-section kinematic model, shows how the adoption of UNI test results for material characterization could be revealed as an unsafe choice for thin slabs.

As it will be mentioned in the final discussion, this evidence could be partially explained by Weibull's theory (Weibull 1951), that relates the specimen volume with the probability that a defect takes place.

Finally, the comparison with fixed-end uniaxial tension test (Fig. 5) confirms the identification procedure adopted, even if for high-carbon steel fiber the linear post-cracking model cannot reproduce at best the residual stress behavior, that needs essentially a bilinear model (di Prisco et al., in press). It is worth noting that the post-cracking constitutive behavior identified by means of bending test appears as an upper bound for tensile tests. This observation introduces some doubts on the real equivalence of identification procedures based on bending or uniaxial tension tests, for significant crack opening.

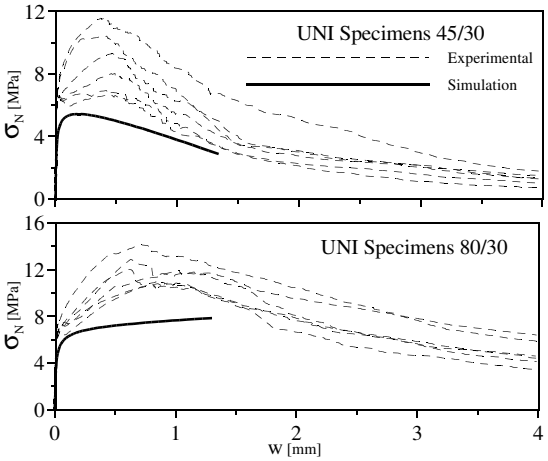

Figure 4. 4-point bending on notched beams (UNI tests)

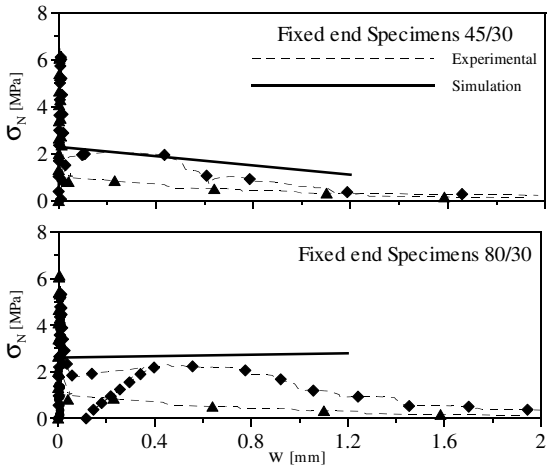

Figure 5. Fixed-end uniaxial tension tests.

2.2 *Experimental set-up for size-effect tests*

The central notched specimens are characterized by three sizes. The notch length (notch ratio = 0.20; Fig. 6) is scaled to the specific size and its shape is introduced to reproduce a defect in a single strip located in the horizontal slab of the roof precast element. The set-up is shown in Figure 6: a rotating-platen device is obtained by coupling three pivot hinges at each end. One of the hinges can be located at a fixed eccentricity of 60 mm. Two sizes of loading device were adopted to reduce the influence of dead loads in the smallest specimens.

The mechanical clamping device is fixed to a closed-loop INSTRON 8562 electromechanical press with a maximum load capacity of 100 kN, for small and medium size specimens and for bending of large size specimens. A closed-loop 2200 kN MTS hydraulic press was used only for uniaxial tension and eccentric tension of the large size specimens. The whole set of tests was strain controlled. The feedback signal was the average of CMOD measures on the symmetry plane for uniaxial tension, the average on stretched side for eccentric tension and the central CMOD of the stretched side for pure bending.

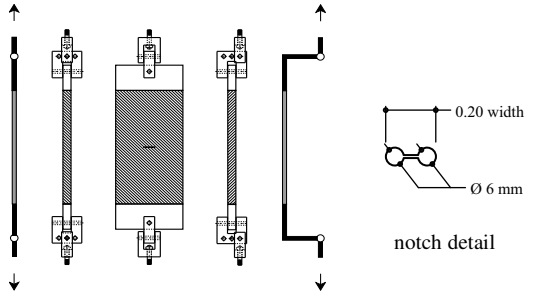

Figure 6. Load set-up for uniaxial and eccentric tension tests.

The selected displacement rate ranged between 0.5 and 1 mm/s with the only exception of small specimen in tension 0.05 (mm/s). The gage lengths of the displacement control were 10 - 120 mm long, while the Crack Opening Displacement gage was always close to 50 mm with the only exception of largest tension test (120 mm).

3 EXPERIMENTAL RESULTS

3.1 *Uniaxial tension*

Also in this case the linear model represents an upper bound for experimental tests (Fig. 7).

The results for large size specimens are not shown because only the peak values are available because of the loss of test-control. They can be observed in Figure 12. The theoretical curve is not at all affected by size effect, because the structural characteristic length has been assumed equal to the thickness of the plate, that is constant. By contrast experimental curve are affected by size-effect: the comparison shows a significant reduction of the peak strength for both the materials and a negligible effect on residual stress. It is worth noting that the residual strength takes advantage of size growth, because the average values are less affected by the local inhomogeneity of fiber density.

Finally the crack propagation into the critical section deserves a comment, because it exhibits some instabilities induced by the central location of the notch and the not homogeneous distribution of steel fiber in the matrix.

The crack first propagates towards the lateral sides (step 1; Fig. 8a, b), then proceeds from front to rear (step 2; Fig. 8a, b).

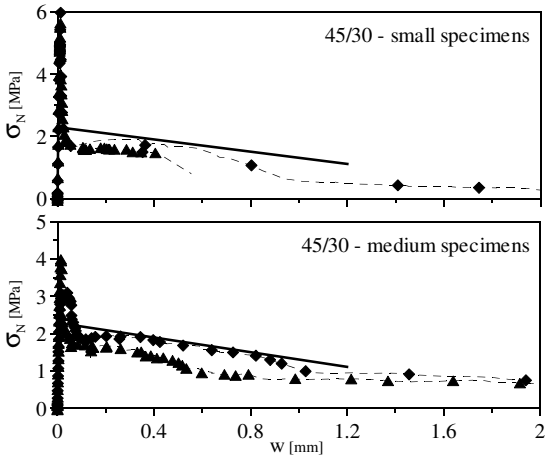

Figure 7. Test results on notched plates: uniaxial tension.

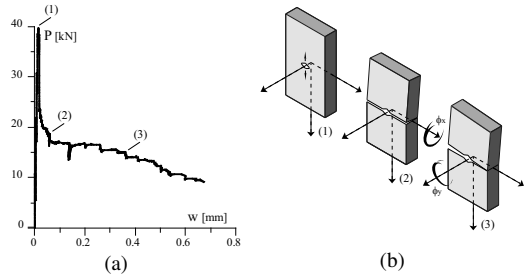

Figure 8. Crack propagation in uniaxial tension tests.

When the peak of post-cracking hardening is reached a local instability denounces the growth of the in-plane rotation typical of rotating-platen uniaxial tension tests (step 3; Fig. 8a, b).

3.2 *Eccentric tension*

Eccentric tension tests confirm two distinct size effects for peak and residual strength (Fig. 9). Also in this loading condition, the simple theoretical model does not take into account any size-effect because for all plate sizes the thickness is 60 mm.

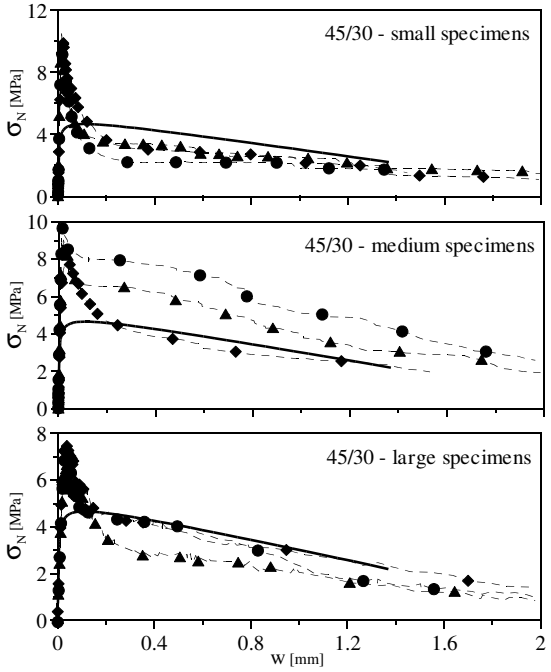

Figure 9. Test results on notched plates: eccentric tension.

The peak of the matrix exhibits a pronounced progressive reduction at growing size, while residual strength seems scantly affected by specimen size, especially the high-carbon steel fiber. Also these tests were partially affected by the crack propagation instabilities observed in uniaxial tension tests.

3.3 *Pure bending*

Bending tests were carried out only on medium and large specimens (Fig. 10) because the small size specimen was not considered significant in order to identify the constitutive behavior, and its geometry would have needed special care to fit instrumental equipment.

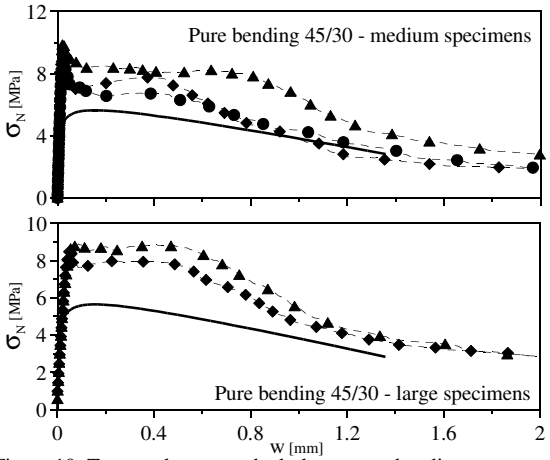

Figure 10. Test results on notched plates: pure bending.

Once again, the theoretical curve used here as a reference, is not affected by any size effect. The tests were easily controlled and confirmed the expected size-effect of the peak strength for the matrix, while no significant size effect was observed in the post-cracking behavior.

Finally, to confirm the effect of increasing specimen size also on unnotched tests, three large size plates (600 × 1900 × 60 mm) made of low-carbon steel fiber were loaded on the span thirds with very stiff load rollers, keeping the load spacing equal to the plate width. The results show a negligible difference with respect to smaller sized plates used for identification procedure. Only one test shows an increased toughness, due to an oblique crack propagation. The same occurred for smaller sized specimens (Fig. 3a, c).

4 DISCUSSION OF RESULTS

The experimental program aims to investigate size effect in SFRC structures when subjected to uniaxial tension, eccentric tension and pure bending. Although the specimens were notched, their peak values were not significantly affected by the notch. Therefore, the results give a measure of the brittleness shown by the materials.

Of course in the problem analyzed the beam depth is always constant and so is the crack open-

ing at the bottom side for an assigned limit crack rotation. When the beam depth grows the ductility progressively reduces because of the limited crack opening able to guarantee a residual strength.

The specimens exhibit a matrix peak strength which is affected by a low scatter (Fig. 11). The strength reduction mainly follows the deterministic size effect. This is confirmed by the good fitting of the experimental tests loaded in eccentric tension for both the materials obtained with the classical size effect law proposed by Bažant (2002; Fig. 11). The nominal strength, defined as specified in Equation 2 is reduced according to Equation 3:

$$\sigma_{max} = \frac{N_{max}}{A}\left(1+\frac{6e}{h}\right) = 7\cdot\frac{N_{max}}{A} = \sigma_N \qquad (2)$$

$$\sigma_N = \frac{\sigma_0}{\sqrt{1+\frac{d}{d_0}}} \qquad (3)$$

the parameters σ_0 and d_0 are computed by means of a linear regression on experimental results.

Residual strength of purely bent specimens is very weakly affected by specimen size (Fig. 12). On the contrary, the smallest size specimens exhibit lower strengths at increasing tensile force *N*, probably because of the larger effect of fiber distribution scatter in a relatively limited cross-section. This evidence is less pronounced in the case of high-carbon steel fiber, thanks to the higher number of thinner fiber. The large scatter of residual strengths (close to ±25%) suggests the adoption of the Weibull's theory of statistical defects. This theory could also be used to justify the differences between the mechanical behavior of notched and unnotched specimens. To this end the critical volume has been considered as the damaged volume astride the notch for the notched tests or the volume between the load rollers for the unnotched tests. According to this procedure, a ratio of about 1.3 ÷ 1.5 on the residual strength has been found in favor of the notched tests.

Further tests recently carried out confirm a larger scatter for UNI tests and a higher residual strength with respect to unnotched bending tests for thin plates. The interaction domains shown in Figure 13 highlight a convex shape for residual strengths which guarantees a safety coefficient for the design when a linear interaction is taken into account. However, when the whole cross section is stretched (i.e. small eccentricity), a further strength reduction would be recommended in order to take into account the reduced ductility.

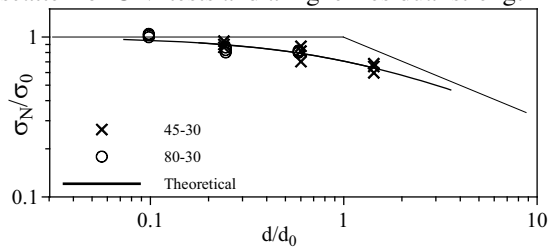

Figure 11. Comparison with size-effect law (Bažant, 2002)

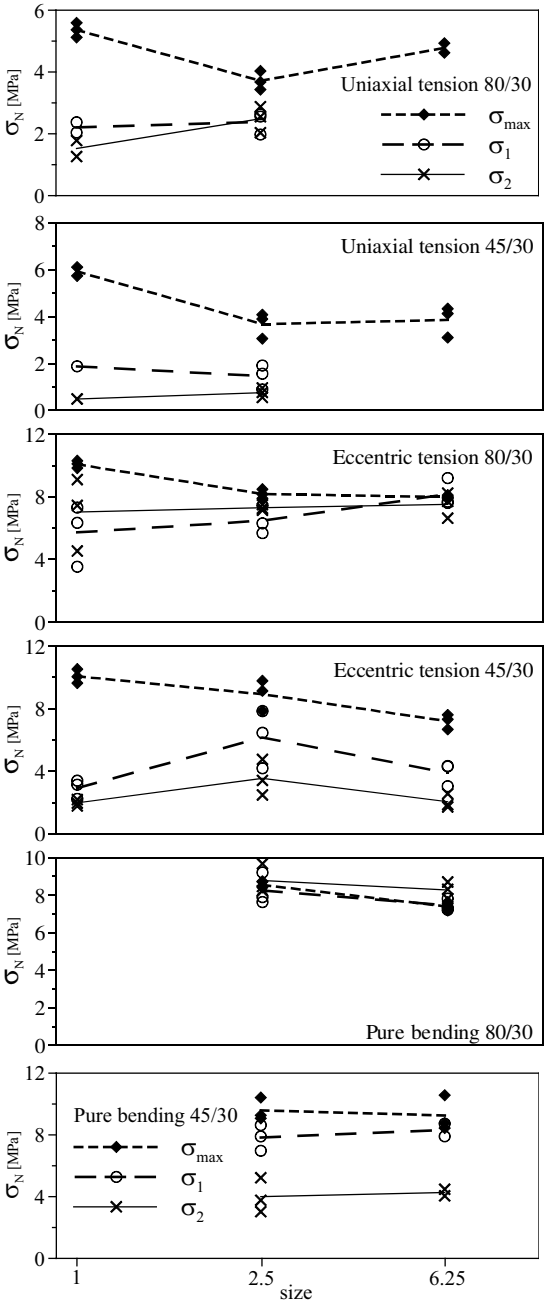

Figure 12. Size-effect on nominal strength.

The theoretical ultimate values N_u and M_u are computed by assuming a rigid plastic behavior and a compression concentrated force applied at the extrados level.

The reference stress σ_2 (defined in paragraph 1.3) has been adopted as the constant plastic stress in the normalization procedure ($M_u = \sigma_2 \cdot bh^2/2$; $N_u = \sigma_2 \cdot bh$).

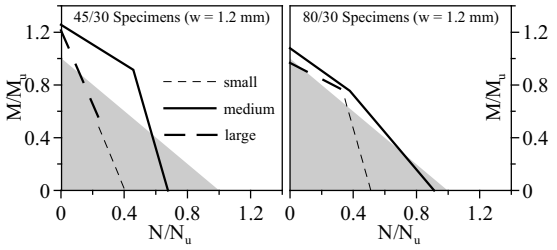

Figure 13. Experimental and theoretical M-N interaction domains.

5 CONCLUSIONS

The design of SFRC thin webbed precast roof elements requires a deepening on the effect of size in thin plates subjected to eccentric tension.

This investigation confirms the reliability of the size effect law proposed by Bažant for the matrix strength, but at the same time shows a negligible size-effect for the residual strength. Therefore, for SFRC bent structures we can expect an increase of ductility at growing of structural size, as in r/c elements characterized by a geometrical reinforcement ratio larger than the minimum one.

Further investigations have ascertained a strong influence of the cast direction on the bending behavior, because the packed fibers tend to concentrate on the bottom side, close to the formworks. Unfortunately, in the tests on real-size structures a negative bending moment was applied, preventing a ductile failure mechanism.

In uniaxial tension tests, the effects of boundary conditions (fixed or rotating-plate ends) on residual strength is almost negligible, if compared with the difference shown by the constitutive laws indirectly determined from bending tests.

The results suggest the identification of the constitutive law in tension directly from an unnotched 4-point bending test, in order to design thin plates taking into account the cast direction. As a matter of fact, fiber distribution and statistical dispersion can drastically alter the benefit expected because of the favorable orientation factor.

6 ACKNOWLEDGEMENTS

The authors thank Magnetti Larco-Building S.p.A. (Carvico, BG, Italy) for its financial and technical support. A special acknowledgment goes to Ing. Claudio Failla, the Technical Director, for the outstanding organization of the whole research project. The authors would also like to thank Ing. Caterina Trintinaglia for her precious support in the experimental tests on real size structure.

7 REFERENCES

Bažant, Z. P. 2002. Reminiscences on Four Decades of Struggle and Progress in Softening Damage and Size Effects. *Concrete Journal* 40 (2): 16-28.

Bažant, Z. P. & Novak, D. 2003. Stochastic models for deformation and failure of quasibrittle structures: recent advances and new directions. In Bicanic et al. (eds.), *Computational Modelling of Concrete Structures*, Swets & Zeitlinger, Lisse, 583-598.

di Prisco, M. 2000. Design of SFRC precast roof elements. In M. di Prisco and G. Toniolo (eds.), *Structural Applications of steel fibre reinforced concrete; Proc. intern. workshop*, *Milano 4 April 2000*, Milan: CTE Press, 33-53.

di Prisco, M., Failla, C., Felicetti, R. & Iorio**,** F. 2000a. HPS-FRC Pprecast roof elements: experimental results and design problems (in Italian). *Studi e Ricerche* 21: 55-93.

di Prisco, M., Felicetti, R. & Iorio, F. 2000b. FRHPC Precast roof elements: from constitutive to structural behavior in bending. In P. Rossi and R.Chanvillard (eds.), *BEFIB; Proc. of the Fifth RILEM Symp. on Fibre Reinforced Concrete*, *Lione, September 2000*, Cachan: RILEM Publications S.A.R.L., 233-243.

di Prisco, M., Felicetti, R., Iorio, F. & Gettu, R. 2001. On the identification of SFRC tensile constitutive behavior. In R. de Borst, J.Mazars, G. Pijaudier-Cabot & J.*G.M. van Mier (eds.), Fracture Mechanics of Concrete Structures, A.A. Balkema Publishe*rs, 541-548.

di Prisco, M., Iorio, F., Trintinaglia, C., Signorini, S. 2002. Thin-web open-section roof elements: geometrical non linearity effects (in Italian), *Proceedings 14° CTE Conference, Mantova*, 569-578.

di Prisco, M., Iorio, F. & Plizzari, G. 2003. HPSFRC prestressed roof elements. In B. Schnütgen and L. Vandewalle (eds.), *Test and Design Methods for Steel Fibre Reinforced Concrete – Background and Experiences,*Bochum: Rilem Publications S.A.R.L., 161-188.

di Prisco, M., Felicetti, R. & Iorio**,** F. in press. Bending behavior of HPC thin-web elements (in Italian), In M. di Prisco and G. Plizzari (eds.), *Fibers and HPC in Structural Applications; Proc. of the IGF National Conf.*, Brescia, 2001.

Ferrara, L. & di Prisco, M. 2001. Three - vs. four-point bend tests: a numerical investigation on plain concrete. *Studies and Research 22*: 73-119.

Lamperti, M. & Menotti, G. 2002. Pprecast SFRC Roof elements: size-effect role (in Italian) Ms. Thesis, Politecnico di Milano, supervised by M. di Prisco and R. Felicetti.

van Vliet, M.R.A. 2000. Size effect in tensile fracture of concrete and rock. Ph. D. Thesis, TU Delft, supervised by J. Van Mier.

Weibull, W. 1951. A statistical theory of the strength of materials. *Journal of Applied Mechanics* 18 (9): 293-297.